

X-raying the ejecta of Supernova 1987A

J. Larsson¹, C. Fransson¹, G. Östlin¹, P. Gröningsson¹, A. Jerkstrand¹, C. Kozma¹, J. Sollerman¹, P. Challis², R. P. Kirshner², R. A. Chevalier³, K. Heng⁴, R. McCray⁵, N. B. Suntzeff⁶, P. Bouchet⁷, A. Crotts⁸, J. Danziger⁹, E. Dwek¹⁰, K. France¹¹, P. M. Garnavich¹², S. S. Lawrence¹³, B. Leibundgut¹⁴, P. Lundqvist¹, N. Panagia^{15,16,17}, C. S. J. Pun¹⁸, N. Smith¹⁹, G. Sonneborn¹⁰, L. Wang²⁰, J. C. Wheeler²¹

¹*Department of Astronomy, The Oskar Klein Centre, Stockholm University, 106 91 Stockholm, Sweden.*

²*Harvard-Smithsonian Center for Astrophysics, 60 Garden Street, MS-19, Cambridge, MA 02138, USA.*

³*Department of Astronomy, University of Virginia, Charlottesville, VA 22903, USA*

⁴*Eidgenössische Technische Hochschule Zürich, Institute for Astronomy, Wolfgang-Pauli-Strasse 27, CH-8093, Zürich, Switzerland.*

⁵*JILA, University of Colorado, Boulder, CO 803090-0440, USA.*

⁶*George P. and Cynthia Woods Mitchell Institute for Fundamental Physics and Astronomy, Texas A&M University, Department of Physics and Astronomy, College Station, TX 77843, USA.*

⁷*DSM/IRFU/Service d'Astrophysique Commissariat à l'Énergie Atomique et aux Énergies Alternatives, Saclay, Orme des Merisiers, FR 91191 Gif-sur-Yvette, France.*

⁸*Department of Astronomy, Mail Code 5240, Columbia University, 550 West 120th Street, New York, NY 10027, USA.*

⁹*Osservatorio Astronomico di Trieste, Via Tiepolo 11, Trieste, Italy.*

¹⁰*NASA Goddard Space Flight Center, Code 665, Greenbelt, MD 20771, USA.*

¹¹*Center for Astrophysics and Space Astronomy, University of Colorado, Boulder, CO 80309, USA.*

¹²*225 Nieuwland Science, University of Notre Dame, Notre Dame, IN 465565670, USA.*

¹³*Department of Physics and Astronomy, Hofstra University, Hempstead, NY 11549, USA.*

¹⁴*ESO, Karl-Schwarzschild-Strasse 2, 85748 Garching, Germany.*

¹⁵*Space Telescope Science Institute, 3700 San Martin Drive, Baltimore, MD 21218, USA.*

¹⁶*INAF-CT, Osservatorio Astrofisico di Catania, Via S. Soa 78, I-95123 Catania, Italy.*

¹⁷*Supernova Limited, OYV #131, Northsound Road, Virgin Gorda, British Virgin Islands.*

¹⁸*Department of Physics, University of Hong Kong, Pok Fu Lam Road, Hong Kong, China.*

¹⁹*Steward Observatory, University of Arizona, 933 North Cherry Avenue, Tucson, AZ 85721, USA.*

²⁰*Department of Physics and Astronomy, Texas A&M University, College Station, TX 77844242, USA.*

²¹*Department of Astronomy, University of Texas, Austin, TX 787120259, USA.*

When a massive star explodes as a supernova, substantial amounts of radioactive elements, primarily ^{56}Ni , ^{57}Ni and ^{44}Ti , are produced¹. After the initial flash of light from shock heating, the fading light emitted by the supernova is due to the decay of these elements². However, after decades, the energy for a supernova remnant comes from the shock interaction between the ejecta and the surrounding medium³. The transition to this phase has hitherto not been

observed: supernovae in the Milky Way are too infrequent to provide a young example, and extragalactic supernovae are generally too faint and too small. Here we report observations that show this transition in the supernova SN 1987A in the Large Magellanic Cloud. From 1994 to 2001 the ejecta faded as predicted by radioactive power from ^{44}Ti . After that, the flux started to increase, reaching a level more than twice as high by the end of 2009. We show that this increase is the result of heat deposited by X-rays produced as the ejecta interacts with the surrounding material.

Due to the proximity of SN 1987A (located only 160,000 light years away), we can study the evolution of the supernova (SN) in great detail. The central ejecta are surrounded by a ring of circumstellar material (Fig. 1) that was shed from the star 20,000 years before the explosion in 1987⁴. Since the explosion, the ejecta have been expanding, and now the outer parts of the ejecta are colliding with the ring, causing it to brighten at all wavelengths⁵⁻⁸. The dense, central part of the ejecta contains most of the mass from the disrupted star and acts as a calorimeter for the energy input to the SN. Here we determine the energy input by tracking the energy output with the Hubble Space Telescope (HST).

Because the ejecta are roughly elliptical in projection on the sky we use an elliptical aperture to measure the brightness. To monitor a constant mass of expanding material, we allow the measuring aperture to expand linearly with time. The axes of the aperture are therefore three times larger in 2009 than in 1994 (Fig. 1). Using this aperture, we determined the R-and and B-band light curves of the ejecta, as shown in Fig. 2 (see Supplementary Table 1 and Supplementary Infor-

mation, section 1 for further details of the observations and light curves). Our measurements show that the flux from the ejecta decays during the first $\sim 5,000$ days after the explosion, as expected from radioactive input, but then starts to increase, reaching a level that is 2-3 times higher around day 8,000 (end of 2009). A new energy source must be present in addition to radioactive decay. Below, we consider a model for the declining phase and then discuss the new energy source that is responsible for the observed increase in flux.

The energy input to the declining phase of the light curve after $\sim 1,500$ days is expected to come from positrons produced in the decay of $^{44}\text{Ti}^{2,9,10}$. To test this we use a model² with abundances taken from the 14E1 explosion model¹¹ and a ^{44}Ti mass of $1.4 \times 10^{-4} M_{\odot}$ ¹² (Supplementary Information, section 3). The model is shown in Fig. 3 together with the observed broadband luminosities. The good agreement with the observations up to day 5,000 confirms that the ^{44}Ti positrons provide the energy input up to this point. However, after day 5,000 the model clearly fails to describe the light curve; radioactive decay cannot explain the increase in flux that we observe.

One possible origin for the flux increase is the reverse shock that results from the interaction between the ejecta and the H II region inside the ring¹³⁻¹⁶. The reverse shock produces strong Ly α and H α emission, which has increased by a factor of ~ 1.7 between 2004 and 2010¹⁶. Although most of this emission originates close to the ring, there is also a component of projected high-velocity H α -emission that can be traced to the central parts of the ejecta¹⁶, which would contribute to the flux we measure. To determine the contribution from the reverse shock to our light curves

we have examined HST STIS spectra from 2004 and 2010 (Supplementary Information, section 2 and Supplementary Fig. 5). The reverse shock can be isolated in the spectra because of its boxy line profile, allowing us to place a limit on its contribution at $\lesssim 20\%$. Furthermore, this changes only marginally between 2004 and 2010, as the expanding measuring aperture remains well inside the area where most of the shock emission is seen. Importantly, an increase in flux is also seen in the [Ca II] $\lambda\lambda 7292, 7324$ lines between 2000 – 2010 (determined from UVES observations at the ESO/VLT, Fig. 2). These lines have velocities $\lesssim 5,000 \text{ km s}^{-1}$, implying that they originate in the inner ejecta (the projected ejecta velocity near the edge of the ring is $\gtrsim 7,000 \text{ km s}^{-1}$ at the present time). We conclude that the increase in flux occurs primarily in the inner ejecta and cannot be explained by emission from the shock region.

We believe that the strong X-ray flux produced in the ring collision is the dominant source of energy input to the ejecta. The X-ray flux from the ring increased by a factor ~ 3 in the 0.5 – 10 keV band between day 6,000 and day 8,000⁶, similar to what we find for the optical emission from the ejecta. To investigate this, we calculated the fraction of X-rays absorbed by the ejecta from a point source located at the ring, using the partially mixed 14E1 explosion model¹⁷. As shown in Supplementary Fig. 6, most of the observed X-ray flux is absorbed in the core region of the ejecta (corresponding to velocities less than $5,000 \text{ km s}^{-1}$), where most of the heavy elements reside. At an energy of $\sim 0.35 \text{ keV}$, which corresponds to the temperature of the dominant component in the X-ray spectrum¹⁸, the fraction of flux absorbed by the ejecta at t_{yr} years can be approximated by $1.6 \times 10^{-3} t_{\text{yr}}^{1.67}$ (the increase with time is mainly due to the increasing solid angle of the expanding ejecta, assumed to be spherical, as seen from the ring). This gives a current-day absorbed X-

ray luminosity of $\sim 5.0 \times 10^{35} \text{erg s}^{-1}$. In this calculation we have neglected the weaker, hard component that contributes to the X-ray spectrum¹⁸. We note that this does not significantly affect the estimate of the absorbed flux, although the hard X-rays may be important due to their larger penetrating power.

To model the ejecta light curve produced by input from the X-rays we scaled the observed X-ray flux⁶ by the fraction absorbed at 0.35 keV, multiplied the resulting flux with a constant (corresponding to the conversion efficiency from X-rays to optical) and added this to the radioactive energy input. Fig. 3 shows the scaled X-ray flux together with the observed light curves. This model follows the general trend of the observed fluxes in both bands, although we note that a more accurate model would need to take into account the detailed shape of the X-ray spectrum and the reprocessing of the X-rays into optical emission. The required conversion efficiency from X-rays to optical emission in our model is 5.0% in the R-band and 3.1% in the B-band.

The conversion of X-rays to optical/IR emission is similar to that of the ⁴⁴Ti positrons. Both involve degradation of non-thermal electrons to heating, ionization and excitation. For a typical ionization fraction of $10^{-3} - 10^{-2}$, the expected efficiency of conversion from X-rays to H α (the dominant line in the R-band) is $\sim 5\%$ (Supplementary Information, section 3). This conversion factor is consistent with the scaling factor we used to model the light curve. Similar arguments apply to the B-band. Furthermore, the density in the core is high enough for the time-scale of recombination to be shorter than the expansion time-scale, ensuring a balance between the energy input and output.

Other possible explanations for the increase in flux include input from a central pulsar¹⁹, a transition from optically thick to optically thin dust and positron leakage from the Fe-rich regions. We find that input from a pulsar is unlikely for several reasons. In particular, it would be a strange coincidence for the emission from the pulsar to mimic the increasing X-ray flux from the ring interaction. Also, we expect the energy input from a pulsar to be concentrated toward the low-velocity material at the centre of the ejecta, while observations of the H α and [Ca II] lines show that the increase occurs for velocities up to $\sim 5,000 \text{ km s}^{-1}$. We also note that constraints on a point source at the centre of SN 1987A have already been obtained using HST data taken near the minimum of the ejecta light curve²⁰. A change in the properties of the dust or a transition in the positron deposition process are also unable to quantitatively explain the observed increase in flux (Supplementary Information, section 4).

We conclude that SN 1987A has made a transition from a radioactively dominated phase to a phase dominated by the X-ray input from the ring collision. This conclusion has interesting implications for the observed morphology. In particular, most of the X-rays are likely to be absorbed at the boundary of the ejecta core, where the density increases rapidly. This may lead to the light from the ejecta being emitted in a ring that is concentrated to the plane of the circumstellar ring. The 'hole' in the ejecta (Fig. 1), which has become more pronounced since ~ 2001 , may in fact be a result of this, rather than reflect the true density distribution or dust obscuration. The asymmetric morphology seen at velocities $\lesssim 3,000 \text{ km s}^{-1}$ in the near-IR [Si I] and [Fe II] lines²¹ is, however, likely to be intrinsic to the metal core. By studying future changes in the morphology of the ejecta, we will be able to understand the origin of this asymmetry

In the future the density of the ejecta will decrease and the fraction of X-rays absorbed will grow (Supplementary Fig. 7). As a result the ionization will increase and a smaller fraction of the X-ray flux will produce line excitation, while a larger fraction will go into heating, leading to an increase in the mid-IR flux and a flattening of the optical light curves. With time the X-rays will also penetrate deeper layers of the ejecta, thereby allowing us to probe the chemical structure of the innermost ejecta. This will be a novel form of X-ray tomography.

References

- [1] Woosley, S. E., Heger, A. & Weaver, T. A. The evolution and explosion of massive stars. *Reviews of Modern Physics* **74**, 1015–1071 (2002).
- [2] Fransson, C. & Kozma, C. Radioactivities and nucleosynthesis in SN 1987A. *New Astronomy Review* **46**, 487–492 (2002).
- [3] McKee, C. F. in *Young Supernova Remnants* (eds S. S. Holt & U. Hwang) vol. 565 of *American Institute of Physics Conference Series*, 17–28 (2001).
- [4] Morris, T. & Podsiadlowski, P. The Triple-Ring Nebula Around SN 1987A: Fingerprint of a Binary Merger. *Science* **315**, 1103–1105 (2007).
- [5] Gröningsson, P. *et al.* Time evolution of the line emission from the inner circumstellar ring of SN 1987A and its hot spots. *Astron. Astrophys.* **492**, 481–491 (2008).
- [6] Racusin, J. L. *et al.* X-ray Evolution of SNR 1987A: The Radial Expansion. *Astrophys. J.* **703**, 1752–1759 (2009).
- [7] Zanardo, G. *et al.* Multifrequency Radio Measurements of Supernova 1987A Over 22 Years. *Astrophys. J.* **710**, 1515–1529 (2010).
- [8] Dwek, E. *et al.* Five Years of Mid-infrared Evolution of the Remnant of SN 1987A: The Encounter Between the Blast Wave and the Dusty Equatorial Ring. *Astrophys. J.* **722**, 425–434 (2010).

- [9] Timmes, F. X., Woosley, S. E., Hartmann, D. H. & Hoffman, R. D. The Production of ^{44}Ti and ^{60}Co in Supernovae. *Astrophys. J.* **464**, 332–341 (1996).
- [10] Diehl, R. & Timmes, F. X. Gamma-Ray Line Emission from Radioactive Isotopes in Stars and Galaxies. *PASP* **110**, 637–659 (1998).
- [11] Shigeyama, T. & Nomoto, K. Theoretical light curve of SN 1987A and mixing of hydrogen and nickel in the ejecta. *Astrophys. J.* **360**, 242–256 (1990).
- [12] Jerkstrand, A., Fransson, C. & Kozma, C. The ^{44}Ti -powered spectrum of SN 1987A. *Astron. Astrophys.* (in press); preprint at <http://arxiv.org/abs/1103.3653> (2011).
- [13] Michael, E. *et al.* Hubble Space Telescope Observations of High-Velocity $\text{Ly}\alpha$ and $\text{H}\alpha$ Emission from Supernova Remnant 1987A: The Structure and Development of the Reverse Shock. *Astrophys. J.* **593**, 809–830 (2003).
- [14] Smith, N. *et al.* The Reverse Shock of SNR 1987A at 18 Years after Outburst. *Astrophys. J.* **635**, L41–L44 (2005).
- [15] Heng, K. *et al.* Evolution of the Reverse Shock Emission from SNR 1987A. *Astrophys. J.* **644**, 959–970 (2006).
- [16] France, K. *et al.* Observing Supernova 1987A with the Refurbished Hubble Space Telescope. *Science* **329**, 1624–1627 (2010).

- [17] Blinnikov, S., Lundqvist, P., Bartunov, O., Nomoto, K. & Iwamoto, K. Radiation Hydrodynamics of SN 1987A. I. Global Analysis of the Light Curve for the First 4 Months. *Astrophys. J.* **532**, 1132–1149 (2000).
- [18] Zhekov, S. A., Park, S., McCray, R., Racusin, J. L. & Burrows, D. N. Evolution of the Chandra CCD spectra of SNR 1987A: probing the reflected-shock picture. *Mon. Not. R. Astron. Soc.* **721**, 518–529 (2010).
- [19] Woosley, S. E., Hartmann, D. & Pinto, P. A. Hard emission at late times from SN 1987A. *Astrophys. J.* **346**, 395–404 (1989).
- [20] Graves, G. J. M. *et al.* Limits from the Hubble Space Telescope on a Point Source in SN 1987A. *Astrophys. J.* **629**, 944–959 (2005).
- [21] Kjær, K., Leibundgut, B., Fransson, C., Jerkstrand, A. & Spyromilio, J. The 3-D structure of SN 1987A's inner ejecta. *Astron. Astrophys.* **517**, A51–A60 (2010).
- [22] Chugai, N. N., Chevalier, R. A., Kirshner, R. P. & Challis, P. M. Hubble Space Telescope Spectrum of SN 1987A at an Age of 8 Years: Radioactive Luminescence of Cool Gas. *Astrophys. J.* **483**, 925–940 (1997).
- [23] Lucy, L. B., Danziger, I. J., Gouiffes, C. & Bouchet, P. Dust Condensation in the Ejecta of Supernova 1987A - Part Two. In S. E. Woosley (ed.) *Supernovae*, 82–94 (1991).
- [24] Wooden, D. H. *et al.* Airborne spectrophotometry of SN 1987A from 1.7 to 12.6 microns - Time history of the dust continuum and line emission. *Astrophys. J. Supp.* **88**, 477–507 (1993).

Supplementary Information

Supplementary information accompanies this paper.

Acknowledgments

This work was supported by the Swedish Research Council and the Swedish National Space Board. Support for the HST observing program was provided by NASA through a grant from the Space Telescope Science Institute, which is operated by the Association of Universities for Research in Astronomy, Inc.

Author contribution

J.L. carried out the data reduction and analysis together with G.Ö., P.G., B. L., J.S. and P.C.; C.F. performed the theoretical modelling together with A.J. and C.K.; J.L. and C.F. wrote the paper. R.P.K. is PI for the HST/SAINTS collaboration. All authors discussed the results and commented on the manuscript.

Author information

Reprints and permissions information is available at www.nature.com/reprints. The authors declare no competing financial interests. Readers are welcome to comment on the online version of this article at www.nature.com/nature. Correspondence and requests for materials should be directed to J.L. (josefin.larsson@astro.su.se) or C.F. (claes@astro.su.se).

Figures legends

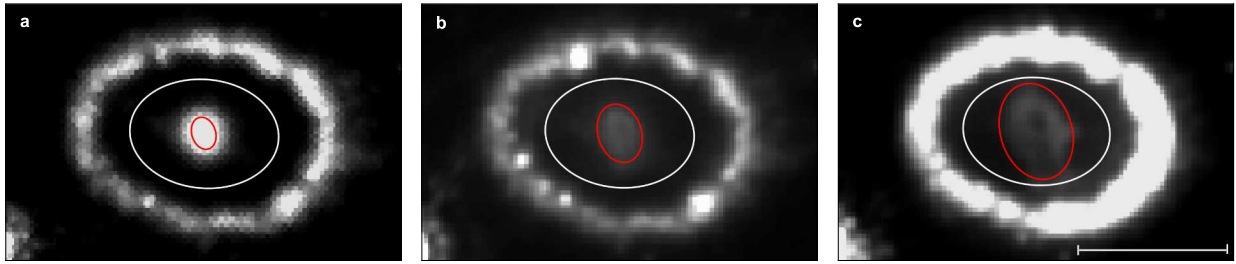


Figure 1: A selection of HST R-band images. The observing dates are 1994-09-24 (**a**), 2000-11-13 (**b**) and 2009-04-29 (**c**), which correspond to 2770, 5012 and 8101 days after the explosion, respectively. The horizontal bar in **c** represents $1''$. The circumstellar ring is inclined at an angle of 45° with respect to the line of sight and is approximately 1.3 light years across. The red (inner) ellipse shows the expanding aperture used for the light curve in Fig. 2. By using an initial semi-major axis of $0.11''$ for the observation in 1994 we always follow the bright, central part of the ejecta without being significantly affected by emission from the circumstellar ring. The white (outer) ellipse shows the fixed aperture used for one of the light curves in Supplementary Fig. 2. The R-band emission from the ejecta is dominated by $H\alpha$ emission with a small contribution from [Ca I-II] lines, while the B-band (Supplementary Fig. 1) is dominated by H I and Fe I-II lines^{12,22}. Note that only the densest, central parts of the ejecta are visible due to the low surface brightness of the outer parts. In reality, the ejecta extend to the ring, as is evident from the strong interaction with the ring.

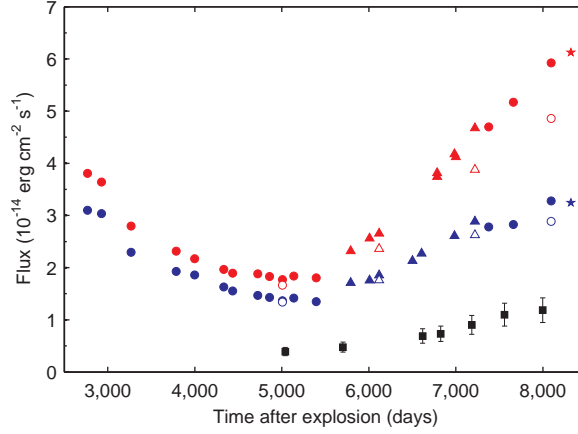


Figure 2: Light curves of the ejecta in different wavebands. Data points from WFPC2, ACS and WFC3 are shown as dots, triangles and stars, respectively. Red and blue symbols correspond to the R- and B-bands. A correction factor has been applied to the ACS and WFC3 fluxes in order to account for the differences between these instruments and WFPC2. To quantify the contamination from the brightening circumstellar ring we created detailed models of the ring for a number of different epochs (Supplementary Information, section 1, and Supplementary Figs. 3 and 4). The open symbols show the ejecta fluxes after the contribution from the ring has been removed. Although the contamination from the ring increases with time it never exceeds $\sim 20\%$ of the flux from the ejecta. The statistical errors on the HST fluxes are smaller than the data points and systematic errors are discussed in the Supplementary Information, section 1. The black squares show the flux of the [Ca II] $\lambda\lambda 7291.5, 7323.9$ lines from VLT/UVES (error bars, s.d.). These lines are free from contamination from the circumstellar ring and the reverse shock. Note the decreasing flux during the first $\sim 5,000$ days and the increase thereafter, indicating an extra source of energy. A further indication that the energy source has changed is that the colour, determined from the flux ratio between the B- and R-bands, changes from a level of ~ 0.8 up to day 5,000 to a value close to ~ 0.6 on day 8,000.

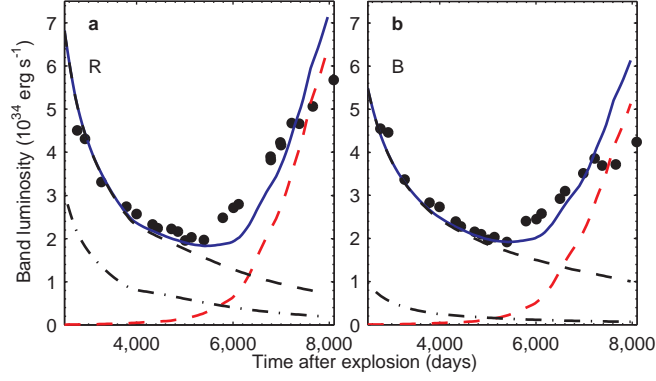


Figure 3: Evolution of the luminosity from the ejecta in the R- and B-bands. The dashed black lines show a model with only radioactive input, mainly from ^{44}Ti . The ^{44}Ti mass used for the model is $1.4 \times 10^{-4} M_{\odot}$ ¹², as determined from a detailed model that takes into account the effects of scattering and fluorescence of the UV flux, as well as a correction for internal dust (here taken to have a 50% covering factor of the core inside 2000 km s^{-1})^{23,24}. The lower dot-dashed lines show the light curves with no ^{44}Ti , illustrating the necessity to include this isotope. The red dashed lines show a model based on a constant fraction of the observed X-ray flux⁶, corrected for the fraction of flux absorbed by the ejecta (Supplementary Fig. 7). The blue solid line shows the sum of both models. The R- and B-bands contain 5% and 3% of the total bolometric flux, respectively, and we expect these fractions to remain roughly constant with time. This is because the relative amount of energy resulting in heating, ionization and excitation will remain nearly constant as long as the ionization by the X-rays is $\lesssim 10^{-2}$. It is clear from this figure that there is a transition at $\sim 5,000$ days from a radioactivity dominated phase to a phase dominated by the X-ray input from the collision with the ring.